ISSN 1047-3289 J. Air Waste Manage. Assoc. 40: 42–46 (1990)

Modeling of Particle Formation and Dynamics in a Flame Incinerator

Virendra Sethi and Pratim Biswas
University of Cincinnati
Cincinnati, Ohio

A model has been developed to predict the formation and growth of metallic particles in a flame incinerator system. Flow fields and temperature profiles in a cylindrical laminar jet flame have been used to determine the position and physical conditions of the species along the flame. The size distribution of the particles formed was approximated by a unimodal lognormal function to describe the aerosol behavior in the flame. The effects of inlet metallic vapor feed concentrations, initial seed sizes and seed concentrations on the resultant particle size distribution are presented. The model has potential for further development to be used as a predictive technique for applications in design and operation of incinerator systems.

Emissions from incineration of hazardous wastes are regulated by the RCRA incinerator performance standards[1] which require a 99.99 percent destruction and removal efficiency for each POHC; a minimum of 99 percent removal of HCl from the exhaust; and particulate emissions less than 180 mg/m^3 of exhaust gases. While the first two requirements are met by most of the incinerators in operation, the particulate emission standards have not been met in many cases.[2] Studies show that waste incineration and coal combustion are the two major contributors to atmospheric loading of toxic metals such as antimony, arsenic, cadmium, selenium, vanadium, lead and zinc.[3] These species are highly volatile and are emitted as enriched submicron-sized particles in the atmosphere which pose a potential health hazard.[4] This problem has been attracting considerable attention lately, especially since the acceptance of waste incineration as a potential alternative to conventional hazardous waste disposal methods. There is a need for effective control and abatement techniques to handle the anticipated increase in the emission levels.[5]

A number of studies have been undertaken in the past to assess the relationship of particle composition and particle size for emissions from coal combustors[4,6] and waste incinerators.[7–9] Flagan et al.[10] and Damle et al.[11] have reviewed the formation of particles in coal combustion and have proposed condensation of vaporized species as a probable mechanism for the formation of submicron-sized particles. It is also well recognized from samples collected that the submicron-sized particles are preferentially enriched with volatile metal species such as antimony, lead, cadmium, silver, copper and zinc.[4,6]

More recently, Barton et al.[12] have carried out an analytical study to predict the fate of toxic metals in waste incinerators. They have concluded that the partitioning of metals during incineration is sensitive to temperature history in the incinerator, chlorine content of the wastes, entrained particle size, residence time and cooling rates downstream of the combustors. In another study, Lee[13] has suggested a thermodynamic approach to predict the chemical and physical form of each species present in the combustion chamber.

The focus of most of the studies till now, has been the assessment of trends from samples collected from incinerators and coal combustors in operation. To better understand and accurately predict metallic particulate emissions from incinerators however, a fundamental study of the mechanism of particle formation and growth is needed. In order to effectively design and choose particle control devices, it is imperative that the particle size distribution of the emissions be known.

A theoretical model is developed in this work to examine particle formation rates and subsequent dynamics in a flame incinerator. The model accounts for physicochemical phenomena and aerosol dynamic effects such as evaporation, nucleation, condensation and coagulation. The model has been used to predict lead particle size distributions for various inlet vapor feed rates and the effects of initial seed size and concentration.

Theoretical Model

The flow field in a laminar cylindrical jet issuing into quiescent air, as shown in Figure 1, is determined from the momentum and energy balance expressions and described by the following equations:[14]

$$\frac{u}{u_i} = F(x, r) \tag{1}$$

$$F(x,r) = \left(1+\frac{48x}{Re_i d_i}\right)^{-1}\left[1-\frac{2r}{d_i}\left(1+\frac{48x}{Re_i d_i}\right)^{-1}\right] \tag{2}$$

$$\frac{v_r}{u_i} = \frac{48r}{Re_i d_i}\left[1+\frac{48x}{Re_i d_i}\right]^{-2}\left[\frac{1}{2}-\frac{4r}{3d_i}\left(1+\frac{48x}{Re_i d_i}\right)^{-1}\right] \tag{3}$$

Implications

The RCRA incinerator particulate emission standards limit the particulate emissions to less than 180 mg/m^3 of exhaust gases. No restriction is currently placed on the chemical (toxicity) and physical (size) characteristics of the particulate emissions. Submicron sized particles pose the greatest environmental (health) hazard. Insufficient data exist on such emissions making it difficult for law and policy makers to formulate effective regulatory strategies. Predictive models such as the one developed, may be used to determine detailed size distributions of emitted aerosols, and hence, provide data to accurately determine risks and extent of adverse health effects. Detailed size distribution data can also be used to design and choose effective particulate control devices and select operating conditions to minimize emissions.

Virendra Sethi is a graduate student and Dr. Pratim Biswas is an Associate Professor in the Department of Civil and Environmental Engineering, University of Cincinnati, Cincinnati, OH 45221-0071. This paper was submitted for peer review on September 1, 1989. The revised manuscript was received on November 13, 1989.

The laminar diffusion flame is modelled by considering a jet issuing into quiescent air. The temperature field $T(x, r)$ for such a diffusion controlled laminar flame burning in an environment with oxygen fraction, Y_o, can be determined from the conservation equations and are written as:

$$T(x, r) = T_o + [(T_i - T_o) - Y_o f\Delta H/C_p]F(x, r) + Y_o f\Delta H/C_p \quad (4)$$

for inside the flame surface, and:

$$T(x, r) = T_o + [(T_i - T_o) + \Delta H/C_p]F(x, r) \quad (5)$$

for outside the flame surface.

The temperature at any location is determined using the cylindrical coordinates calculated from the flow field described above using the following equations for the flame shape and height:

$$\frac{2\delta}{d_i} = \left(1 + \frac{48x}{Re_i d_i}\right) \quad (6)$$

$$x_c = \frac{Re_i d_i}{48 f Y_o} \quad (7)$$

The metal species is introduced coaxially into the flame with the fuel inlet in the jet. High temperatures in the flame may cause the metal species to vaporize completely or partly depending on the initial feed size, and no formation or growth of particles is expected within the flame. As the temperature decreases downstream of the flame, saturation conditions for the vapor are reached and the vapor may either nucleate to form new particles or condense onto existing particles. Further growth may take place by Brownian collisions leading to larger coagulated particles. Particles may also be generated by chemical reaction in the flame under the high temperature conditions, in which case most particles are formed within the flame and further growth is controlled by coagulation beyond the flame. Such particulate formation is typical of most powder production methods that use aerosol reactors. The aerosol dynamics for such a system are described by the General Dynamic Equation (GDE).[15] Assuming that the size distribution of the particles is described by a unimodal lognormal function, the aerosol dynamics can be described by the first three moments of the aerosol size distribution.[16]

The rate of change of the zeroeth moment, M_0 (particle concentration), is given by:[16,17]

$$\frac{dM_0}{dt} = I + kC - \xi M_0^2 \quad (8)$$

The first term on the right hand side accounts for particle formation by nucleation, the second term for particle formation by chemical reaction, and the third term for the loss of particles due to coagulation.

The rate of change of the first moment M_1 (total aerosol volume) is given by:

$$\frac{dM_1}{dt} = Iv^* + \eta(S - 1)M_0 + kCv_1 \quad (9)$$

The first term on the right hand side accounts for increase in aerosol volume due to the formation of the nucleated particles, the second term for volume change by condensation or evaporation, and the third term for the volume increase due to particles formed by chemical reaction.

The rate of change of the second moment, M_2, is given by:

$$\frac{dM_2}{dt} = Iv^{*2} + 2\zeta(S - 1)M_1 + \psi M_1^2 + kCv_1^2 \quad (10)$$

The first term on the right hand side accounts for the change due to nucleation, the second term for the effect of condensation and evaporation, the third term for the effects of coagulation and, the last term for the effects of chemical reaction.

The rate of change of the saturation ratio of the species is determined from vapor balance and is given by:

$$\frac{dS}{dt} = -\frac{Ik^*}{n_s} - \epsilon(S - 1)M_0 + \frac{R}{n_s} \quad (11)$$

The first term on the right hand side accounts for the vapor loss by nucleation of particles, the second term for the change due to condensation or evaporation, and the third

Greek Letters

δ = boundary layer thickness of the jet
ϵ = coefficient of condensation from Equations 13 and 22 (Reference 16)
γ = surface tension
η = coefficient of condensation from equations 11 and 20 (Reference 16)
σ = size deviation
Σ = surface tension group[16] ($=\gamma v_1^{2/3}/k_B T$)
ξ = coeffient of coagulation from Equations 9 and 19 (Reference 16)
ψ = coefficient of coagulation from equations 12 and 21 (Reference 16)
ζ = coefficient of condensation from Equations 12 and 21 (Reference 16)

Nomenclature

C = chemical species concentration
C_p = specific heat capacity of gaseous species
ΔH = enthalpy of combustion
d_i = jet diameter at inlet
d_g = geometric mean diameter
f = number of grams of fuel for 1 gram of oxygen
I = nucleation rate[16] ($=n_s^2 s_1 (k_B T/2\pi m_1)^{1/2} S^2 (2/9\pi)^{1/3} \Sigma^{1/2} \exp(-k^* \ln S/2)$)
k = chemical rate constant
k^* = number of molecules in a critical cluster
k_B = Boltzmann constant
n_s = number of molecules of metal specie at saturation
m_1 = molecular mass of metal specie
M_k = kth moment with respect to volume
R = vapor source rate
r = radial position
r_i = initial radial position
Re_i = Reynold's number at jet inlet
S = saturation ratio
s_1 = surface area of a molecule of metal specie
t = time
$T(x, r)$ = temperature field
T_i = fuel temperature at inlet
T_o = ambient temperature
u = axial velocity component
u_i = axial velocity at jet inlet
v^* = critical molecule cluster volume
v_1 = molecular volume
v_r = radial velocity component
x = axial displacement
x_c = flame height
x_i = initial axial position
Y_o = oxygen mass fraction in ambient

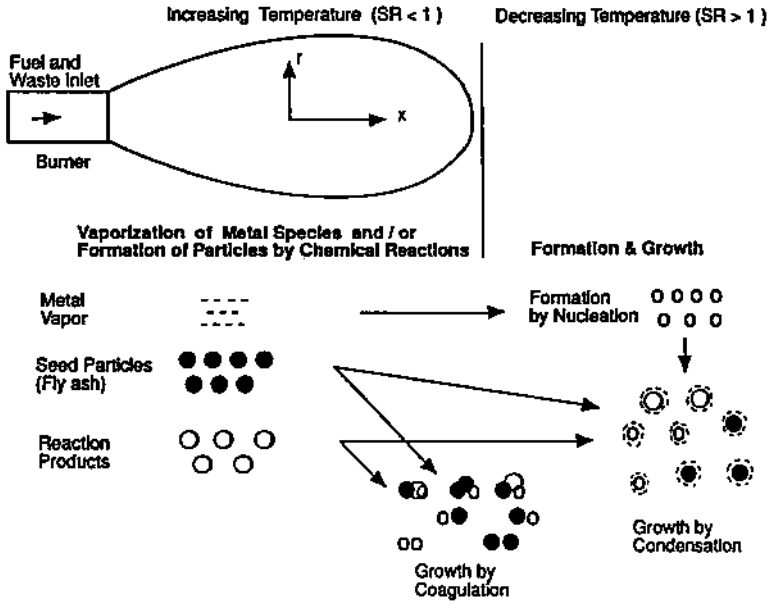

Figure 1. Schematic of the burner showing particle formation and growth mechanisms in the flame.

term for addition from any vapor source. The expressions for the various terms are described in the nomenclature.

Equations 8 through 11 constitute a set of coupled ordinary differential equations that are solved using the Adams-Moulton routine, DGEAR.[18] The evolution of the first three moments M_0, M_1 and M_2 from these equations are sufficient to describe the particle size distribution completely.

Results and Discussion

The model presented above is used to predict the formation of particles from a lead vapor feed introduced coaxially with the fuel gas at the jet inlet. Table I lists the physical conditions of the simulated system.

The particles formed are assumed to follow the fluid streamlines. An initial radial position r_i and axial position x_i (=0) is assumed and the new radial and axial positions are determined using the radial and axial velocity components in Equations 1 and 3 after a small time increment. The procedure is repeated successively to determine the location of the particles in the jet at any time t.

The theoretical temperature profile $T(x, r)$, is determined for three initial radial positions of r = 0, 0.05 and 0.1 cm and are plotted as a function of axial displacement in Figure 2.

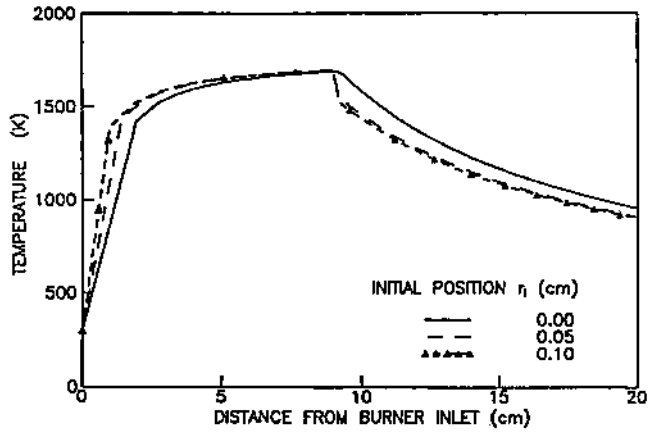

Figure 2. Theoretically predicted flame temperature for initial radial positions: r_i = 0, 0.05 and 0.1 cm.

The effect of feed rate of lead vapor on the formation and growth of lead particles is shown in Figure 3. The feed rates used are typically in the range of those encountered in an incinerator operation (a 210-kg/week of lead[8] is equivalent of 7.2×10^7 $\mu g/m^3$ feed concentration simulated in the model). The saturation ratio, S, is an inverse function of the temperature and decreases rapidly with the increasing flame temperatures. No nucleation or condensation effects are expected in the unsaturated vapor conditions prevalent within the flame. Any particles expected to be formed by nucleation within the flame undergo evaporation and disappear completely. The evolution of the number concentration, volume average diameter, and total aerosol volume for vapor feed rates of 10^6, 10^7 and 10^8 $\mu g/m^3$ along the flame axis is plotted in Figure 3. The formation of particles for the 10^8 $\mu g/m^3$ feed rate occurs earlier than that for the lower feed rates as the saturation conditions are reached sooner. Once the particles are formed, they scavenge the vapor (by condensation) thus suppressing nucleation and further increase in particle concentration. For lower feed rates, the number of particles formed initially are insufficient to quench nucleation completely, resulting in higher number concentration than that for the 10^8 $\mu g/m^3$ feed rate. The total volume of lead vapor that has condensed out of the vapor phase is a measure of the upper limit of the collectible particulate from incineration of the wastes. A significant observation may be made: If the vapor feed is high, the particles formed are fewer and larger—a condition that is very desirable for efficient control of emissions. However, if the vapor feed rate is low, the result is

TABLE I. Physical conditions for the system.

Metal species	Lead
Specific gravity	10.1
Surface tension	500 dyn/cm
Molecular weight	207 gm/mol
Flame	
Fuel	Methane
ΔH	210.8×10^3 kCal/mol
C_p	8.3 kCal/mol K
T_i	298 K
T_a	298 K
Y_a	0.232
f	0.25
d_i	0.2 cm

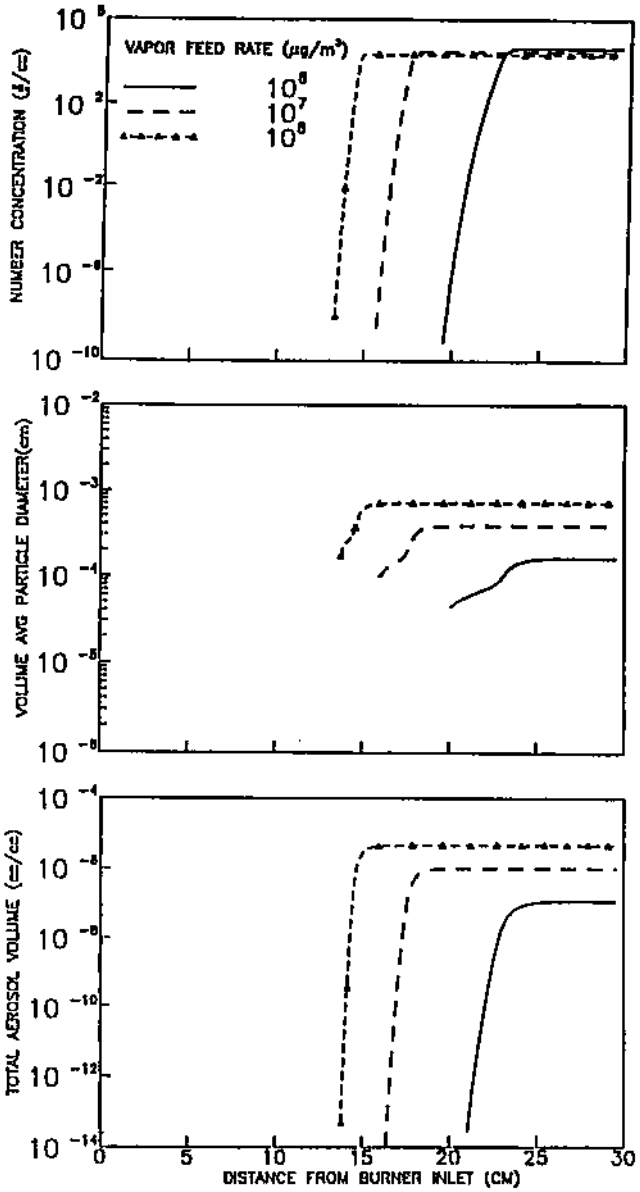

Figure 3. Effect of vapor feed rate ($\mu g/m^3$) on the resultant lead aerosol characteristics along the flame axis ($r = 0$).

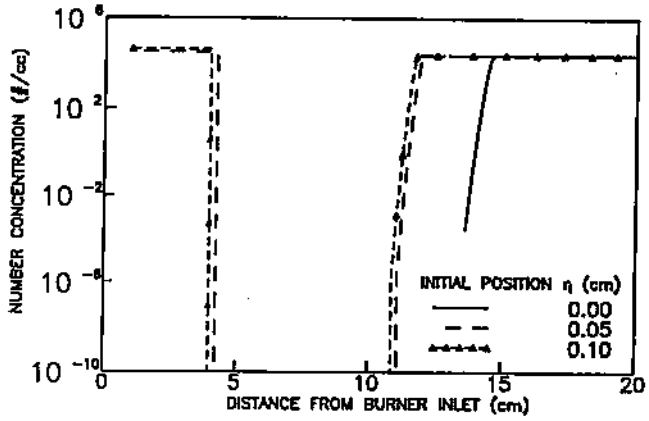

Figure 4. Effect of initial position, r_i, on the resultant lead aerosol concentration along the streamlines for a vapor feed rate of 10^8 $\mu g/m^3$.

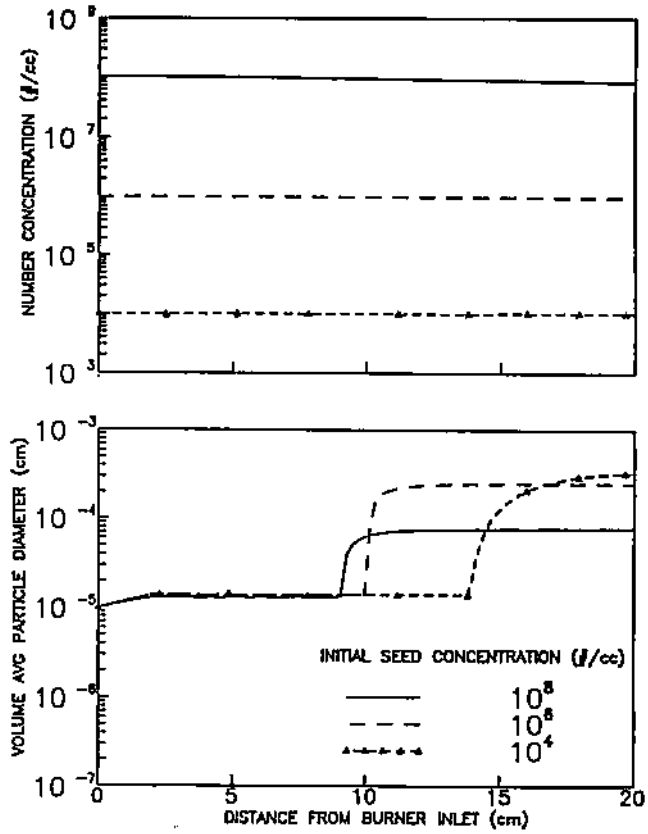

Figure 5. Effect of initial seed concentration on the resultant lead aerosol characteristics for a vapor feed rate of 10^8 $\mu g/m^3$, initial seed diameter of 0.1 μm, and an initial seed geometric standard deviation σ_i of 1.0.

a large number of smaller sized particles which are difficult to collect by control devices. In practice, however, this extremity is partly subdued by the presence of suspended particles that offer surface for vapor to preferentially condense out, a point which we discuss later in this paper.

Since the temperature is a function of axial location, x, and radial position, r, the particle concentration for the streamlines with initial radial positions $r = 0$ (centerline), 0.05 and 0.1 cm (wall) were studied for comparison and are shown in Figure 4 for a vapor feed rate of 10^8 $\mu g/m^3$. It is observed that though the formation of particles at the inlet is significantly affected by the initial radial position, all particles evaporate in the flame and the formation of the particles by nucleation beyond the flame surface is not affected greatly.

Most incinerators will have other particles (such as flyash) present that can act as seed particles for vapor condensation. Typically the flyash particles are nonvolatile (such as SiO_2) and do not affect the vapor balance of the metal species under consideration. The effect of the presence of a monodisperse seed (0.1 μm diameter) at different initial concentrations (10^4, 10^6 and 10^8 #/cc) is shown in Figure 5. Formation of new particles by nucleation is quenched by the preferential condensation of vapor on the seed particles. This is evident from Figure 5: there is an increase in the particle diameter with no change in the number concentration.

The effect of different initial seed size on the resultant lead aerosol characteristics for a constant feed rate of 10^6 $\mu g/m^3$ and seed concentration of 10^6 #/cc is shown in Figure 6. The number concentration does not change as the vapor condenses onto the existing seed particles. The associated increase in particle size indicates that condensational growth dominates. This indicates that seeds may be used to scavenge volatile metal (in vapor state), and then be effectively captured in particle control devices.

The model can be used to simulate more realistic polydisperse seed distributions. A typical flyash size distribution[10] ($M_0 = 10^6$ #/cc, $d_g = 0.1$ μm, and $\sigma = 1.5$) is assumed to be

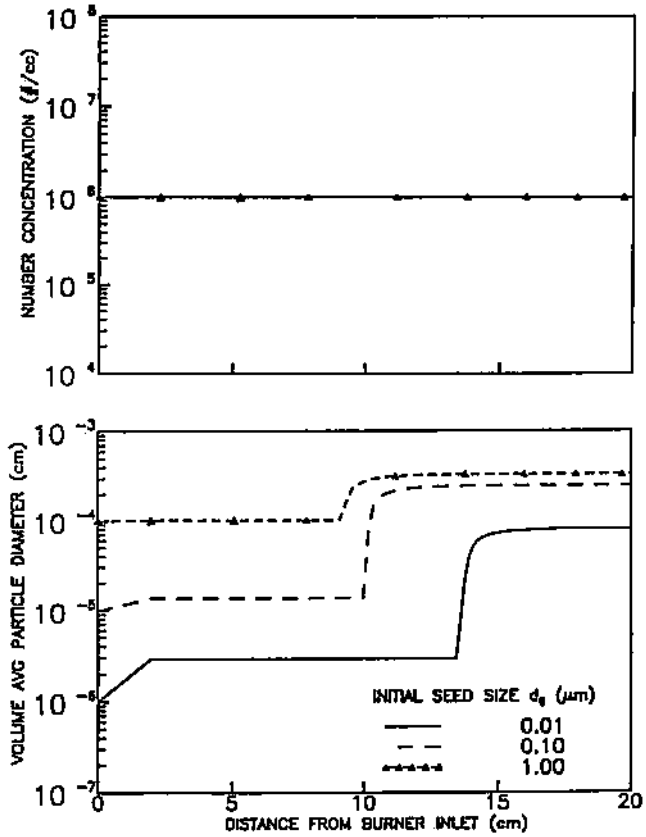

Figure 6. Effect of initial seed size on the resultant lead aerosol characteristics for an initial seed concentration of 10^6 #/cc, standard deviation, σ, 1.0, and a vapor feed rate of 10^6 $\mu g/m^3$.

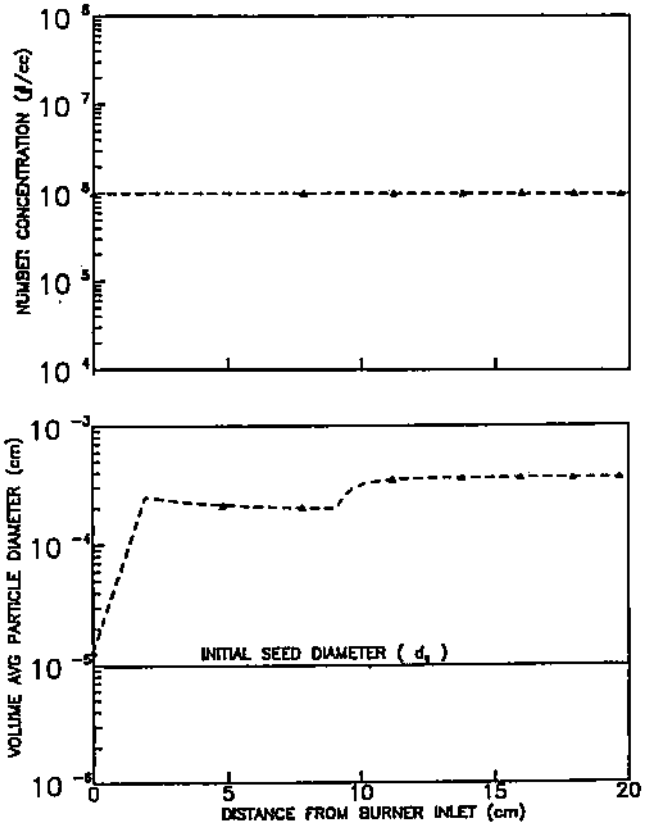

Figure 7. Model results for the characteristics of a lead aerosol formed in a typical incinerator with suspended flyash particle seed concentration of 10^6 #/cc, geometric mean diameter, d_p, of 0.1 μm, geometric standard deviation, σ = 1.5, and a vapor feed rate of 10^6 $\mu g/m^3$.

the seed, and is used to predict resultant lead aerosol characteristics (Figure 7). For a typical lead feed rate of 10^6 $\mu g/m^3$, most of the vapor condenses onto the existing seed particles.

Conclusions

A model accounting for various physicochemical and aerosol dynamic phenomena has been developed to predict volatile metal particle formation in flame systems. The model has been applied to a simple methane-air flame system with a lead vapor feed. The effects of inlet vapor feed rate and seed particles on the resultant lead particle size distributions have been determined. No volatile metal particles are expected to form inside the high temperature flame region. As the temperature decreases downstream, rapid nucleation of the vapor leads to formation of small particles. In the presence of seed particles, condensation is expected to be the dominant mechanism. Controlled experimental tests are being performed to verify the predictions of the model. After verification, this model can be used as a predictive tool in real incinerator systems. It can also be used as a design tool to minimize emissions of toxic volatile elements.

Acknowledgments

Partial support from NSF Grant CBT 8808813 and EPA Contract RTP 42.0 is gratefully acknowledged. This work was presented at the 82nd Annual Meeting of the Air and Waste Management Association held in Anaheim, California, in June 1989.

References

1. "Standards applicable to owners & operators of hazardous waste treatment, storage, and disposal facilities; consolidated permit regulations and the hazardous waste management system," *Federal Register* 47: 27516 (1982).
2. E. T. Oppelt, "Hazardous waste destruction," *Environ. Sci. Tech.* 20: 312 (1986).
3. G. S. Kowalcyzk, C. E. Choquette, G. E. Gordon, "Chemical element balances and identification of air pollution sources in Washington, D.C.," *Atmos. Environ.* 12: 1143 (1978).
4. R. L. Davison, D. F. S. Natusch, J. R. Wallace, C. A. Evans, "Trace elements in fly ash," *Environ. Sci. Tech.* 8: 1107 (1974).
5. E. T. Oppelt, "Incineration of hazardous waste—A critical review," *JAPCA* 37: 558 (1987).
6. E. S. Gladney, J. A. Small, G. E. Gordon, "Composition and size distribution of in-stack particulate material at a coal fired power plant," *Atmos. Environ.* 10: 1071 (1976).
7. R. R. Greenberg, W. H. Zoller, G. E. Gordon, "Composition and size distributions of particles released in refuse incineration," *Environ. Sci. Tech.* 12: 566 (1978).
8. S. L. Law, G. E. Gordon, "Sources of metals in municipal incinerator emissions," *Environ. Sci. Tech.* 13: 432 (1979).
9. R. L. Bennet, K. T. Knapp, "Characterization of particulate emissions from municipal waste water sludge incinerators," *Environ. Sci. Tech.* 16: 831 (1982).
10. R. C. Flagan, S. K. Friedlander, "Particle formation in pulverized coal combustion—A review," *Recent Developments in Aerosol Science*, Chapter 2, John Wiley, New York, 1971.
11. A. S. Damle, D. S. Ensor, M. B. Ranade, "Coal combustion aerosol formation mechanisms: A review," *Aerosol. Sci. Tech.* 1: 119 (1982).
12. R. G. Barton, P. M. Maly, W. D. Clark, W. R. Seeker, "Prediction of the fate of the toxic metals in waste incinerators," submitted ASME 13th National Waste Processing Conference, Philadelphia, May 1988.
13. C. C. Lee, "A model analysis of metal partitioning in a hazardous waste incineration system," *JAPCA* 38: 941 (1988).
14. A. M. Kanury, *Introduction to Combustion Phenomena*, Chapter 7, Gordon and Breach, 1982.
15. S. K. Friedlander, *Smoke Dust and Haze*, Wiley, New York, 1977.
16. S. E. Pratsinis, "Simultaneous aerosol nucleation, condensation and coagulation in aerosol reactors," *J. Coll. Inter. Sci.* 124: 416 (1988).
17. P. Biswas, X. Li, S. E. Pratsinis, "Optical waveguide preform fabrication: Silica formation and growth in a high temperature aerosol reactor," *J. Appl. Phys.* 65: 2445 (1989).
18. "IMSL Contents Document," IMSL, 8th ed., International Mathematical and Statistical Libraries, Houston, 1980.